ACS OMEGA

http://pubs.acs.org/journal/acsodf

Article

Quantum Modification of Indacenodithieno[3,2-*b*]thiophene-Based Non-fullerene Acceptor Molecules for Organic Solar Cells of High Efficiency

Fahed A. Aloufi, Riyadh F. Halawani, Bassem Jamoussi, Amira K. Hajri,* and Nesrine Zahi

Cite This: *ACS Omega* 2023, 8, 21425−21437

Read Online

ACCESS | Metrics & More | Article Recommendations | Supporting Information

ABSTRACT: In order to enhance the efficacy of organic solar cells, six new three-dimensional small donor molecules (**IT-SM1** to **IT-SM6**) have been computationally designed by modifying the peripheral acceptors of the reference molecule (**IT-SMR**). The frontier molecular orbitals revealed that **IT-SM2** to **IT-SM5** had a smaller band gap (E_{gap}) than **IT-SMR**. They also had smaller excitation energies (E_x) and exhibited a bathochromic shift in their absorption maxima (λ_{max}) when compared to **IT-SMR**. In both the gas and chloroform phases, **IT-SM2** had the largest dipole moment. **IT-SM2** also had the best electron mobility, while **IT-SM6** had the best hole mobility owing to their smallest reorganization energy for electron (0.1127 eV) and hole (0.0907 eV) mobility, respectively. The analyzed donor molecules' open-circuit voltage (V_{OC}) indicated that all of these proposed molecules had greater V_{OC} and fill factor (FF) values than the **IT-SMR** molecule. In accordance with the evidence of this work, the altered molecules can seem to be quite proficient for usage by experimentalists and have prospective use in future in the manufacture of organic solar cells with improved photovoltaic properties.

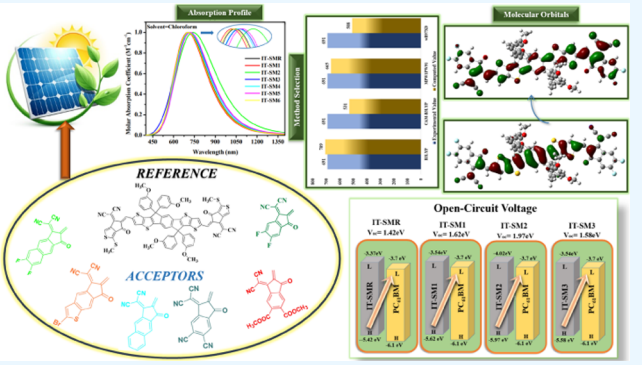

1. INTRODUCTION

Organic solar cells (OSCs) can be employed in a variety of potential implementations due to their affordability, lightness, and capability to be processed in solutions.[1,2] OSCs provide several advantages over silicon solar cells, including a wider variety of active-layer materials, reduced weight, more transparency, and greater pliability. These advantages have elevated OSCs to a position of prominence among solar cell technologies.[3] Improvements in materials science, mechanics, and materials manufacturing have allowed the power conversion efficiency (PCE) of organic solar cells (OSCs) to increase from 11 to 19% during the previous 5 years.[4] The device efficacy of bulk-heterojunction OSCs is affected by the blend of donor and acceptor material in the light-absorbing layer.[4,5] The functionality of fullerene acceptors (FAs) is constrained by a number of important challenges, including concerns with chemical change, unstable morphology, energy levels that are nonupgradable, and weak absorbance in the near-infrared (NIR) as well as UV−visible region. For these reasons, non-fullerene acceptors (NFAs) are preferable to fullerene acceptors (FAs).[6] This suggests that the unending growth of non-fullerene acceptors (NFAs) may be responsible for the 5-year-long upward trend in PCEs of OSC. This rise in the photovoltaic performance of materials based on NFA is credited to their improved light-harvesting efficiency, broad light absorption, and variable energy levels.[7]

Indacenodithieno[3,2-*b*]thiophene (IDTT) is a ladder-type electron-rich backbone used as the middle donor portion in a variety of A−*π*−D−*π*−A- and A−D−A-type chromophores. Tunable optoelectronic characteristics are achieved with high power conversion efficiencies by copolymerizing it with various acceptor units.[8] In particular, it provides a deep-lying highest occupied molecular orbit and a broad band gap for the resultant polymers. As a result, the IDTT-based polymer donors have huge potential as donors in various OSCs. IDTT also offers high hole mobility, outstanding electrochemical stabilities, a notable absorption coefficient, and charge transport kinetics.[9]

Zhan et al. in 2015 efficiently synthesized an IDTT-based NFA called ITIC.[10] The NFA named ITIC showed absorption between 500 and 780 nm. In addition to being highly soluble in a wide range of organic solvents, it also had excellent mobility of electrons. In many investigations, the chemical modifications of ITIC-based acceptors are done to provide significant PCEs of 8−14% for OSCs.[10,11] It exhibited a 678 nm wavelength of maximum absorption in the solution of chloroform and 700 nm

Received: December 14, 2022
Accepted: May 11, 2023
Published: June 7, 2023

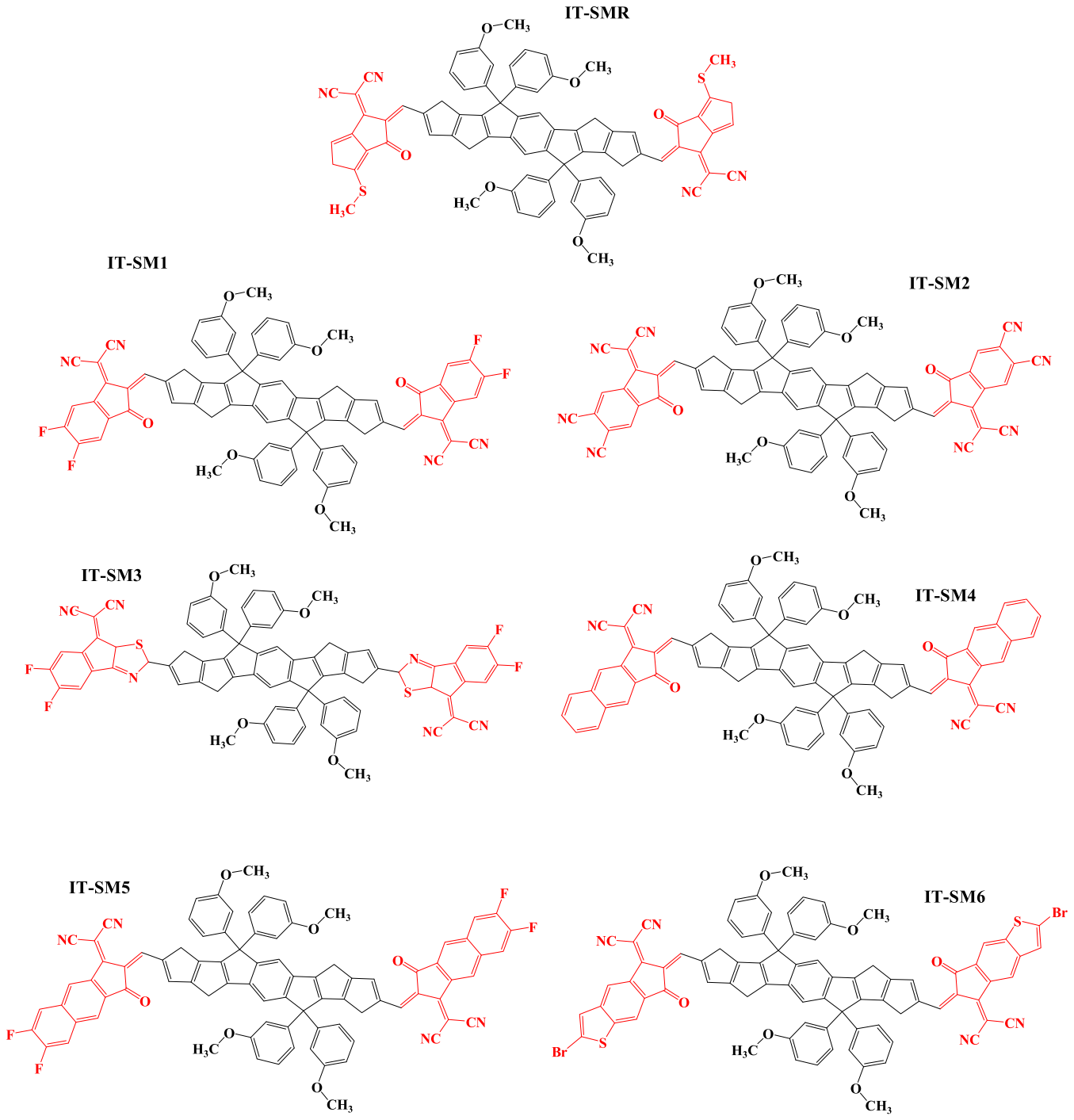

Figure 1. ChemDraw geometries of **IT-SMR** and **IT-SM1** to **IT-SM6** molecules.

in the film with an onset wavelength of 770 nm. Its optical band gap was seen to be 1.61 eV with frontier molecular orbitals at −5.50 and −3.76 eV for the highest occupied and lowest unoccupied orbitals, respectively.[12] The majority of the research mentioned previously made an effort to alter the effect of the end-groups (EGs). Hou et al. used an EG that had been methylated and named the molecule IT-M. The open-circuit voltage (V_{OC}) is raised by the methyl group's poor electron-donating properties, which raise the energy level of LUMO in IT-M. As a result, they were able to achieve a PCE of 12.05%.[12b] Yang et al. changed the benzene ring to thiophene in EGs and gave the molecule a new name ITCPTC.[13] After enhancing the intermolecular forces, crystalline nature, and charge transport of ITCPTC, they found that the fill factor (FF) rose to a notable level.

Researchers have developed a novel class of NFA based on ITIC, dubbed IEICO-4F.[14] The following is a summary of the molecular engineering approaches used in the investigation by Jeong et al. in 2022.[12b] Strengthening the intermolecular forces via sulfur−sulfur linkages was achieved by replacing the benzene ring of EG with thiophene.[15] Modification of the EG is done by incorporating a thiomethyl group into its fused thiophene ring in order to reduce the HOMO energy.[16] To increase the solubility

https://doi.org/10.1021/acsomega.2c07975
ACS Omega 2023, 8, 21425−21437

of the NFAs in normal organic solvents, alkoxy groups were introduced to the meta-phenyl site of the core of the molecule.[17]

In the current computational approach, we have considered IT-SM as our reference molecule (**IT-SMR**). The central region of the reference (**IT-SMR**) is based on IDTT, which is a donor region of the molecule and the acceptor EGs are existing at both terminal sites, i.e., 2-(5-methylene-1-methylsulfanyl-6-oxo-5,6-dihydro-cyclopenta[*c*]thiophen-4-ylidene)-malononitrile. By replacing the **IT-SMR** molecule's terminating acceptor component with six other acceptor groups, we have theoretically developed six novel non-fullerene donor compounds. The new six acceptor groups are 2-(5,6-difluoro-2-methylene-3-oxo-indan-1-ylidene)-malononitrile (**IT-SM1**), 1-dicyanomethylene-2-methylene-3-oxo-indan-5,6-dicarbonitrile (**IT-SM2**), 1-dicyanomethylene-2-methylene-3-oxo-indan-5,6-dicarboxylic acid dimethyl ester (**IT-SM3**), 2-(2-methylene-3-oxo-2,3-dihydro-cyclopenta[*b*]naphthalen-1-ylidene)-malononitrile (**IT-SM4**), 2-(6,7-difluoro-2-methylene-3-oxo-2,3-dihydro-cyclopenta[*b*]naphthalen-1-ylidene)-malononitrile (**IT-SM5**), and 2-(2-bromo-6-methylene-7-oxo-6,7-dihydro-1-thia-s-indacen-5-ylidene)-malononitrile (**IT-SM6**) as shown in Figure 1. These end-caps of the molecules were selected due to their significant conjugation and electron-withdrawing capabilities. Additionally, the acceptors of **IT-SM1** to **IT-SM3** have similar ring skeletons but varying terminal fluoro, cyano, and acetyl groups so that a proper comparison could be done. Similar is the case with acceptors of **IT-SM4** and **IT-SM5**, where the only difference is of the additional fluoro group in the latter molecule. Finally, the acceptor of **IT-SM6** is also known to have prominent conjugation and thus was selected.[18] We have replaced the long alkoxy chains of the molecules with simple methoxy ones, with the assumption that the length of the chain while affecting the solubility does not necessarily affect the photovoltaic attributes of the molecules. This also helped us reduce the computational cost.

2. COMPUTATIONAL ASPECTS

Gaussian 09[19] was used for all of the molecular geometry computations, and GaussView 6.0.16[20] was used to model and see the resulting three-dimensional geometries.[21] DFT[22] simulations were carried out using the B3LYP,[23] CAM-B3LYP,[24] MPW1PW91,[25] and ωB97XD[26] functionals in combination with the 6-31G(d,p) basis set for the optimization of the **IT-SMR**. After optimizing the geometry, we used time-dependent density functional theory (TD-DFT) calculations to predict the light absorption attributes of **IT-SMR**, and we used the integral equation formalism polarizable continuum model (IEFPCM)[27] to explore the solvent (chloroform) impact on these properties. Absorption maxima (λ_{max}) of **IT-SMR** from the aforementioned four functionals was compared to empirical λ_{max} values found in the literature to ensure the viability of the theoretical method. The four estimated values of λ_{max} (709, 531, 665, and 508 nm, respectively) are compared with the experimental λ_{max} of **IT-SMR** (691 nm),[12b] as shown in Figure 2. The Becke, 3-parameter, Lee−Yang−Parr (B3LYP) functional was the one we identified to be most in line with the experimental data, suggesting that calculations with this functional would provide the most accurate results for the theoretically developed compounds.

The absorption spectra of the compounds were created with the aid of Origin 6.0.[28] In order to see how excitons travel and interact, we took readings from a transition density matrix (TDM) and used the Multiwfn program[29] to visualize the data.

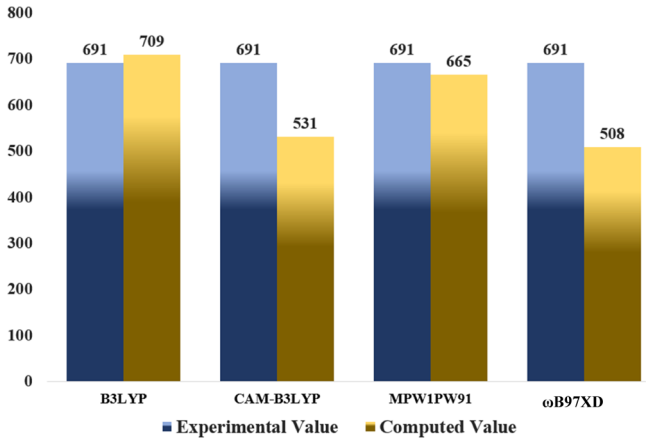

Figure 2. Comparison of **IT-SMR** molecules' computed and experimental λ_{max}.

Graphs depicting the density of states (DOS)[30] were generated using PyMOlyze 1.1.[31] The oscillator strength was evaluated for the studied chromophores, in addition to, the excitation and binding energies, etc.

The Marcus theory was used to calculate the intra- and intermolecular charge mobility by exploring the reorganization energy (RE).[32] The focus of our current work, however, has been on the intramolecular charge transfer (ICT). The term "RE" refers to the combined effects of two separate but related forms of reorganizational forces. Internal RE is mostly dependent on variations in molecular structure, whereas external RE is subject to rapid oscillations in the outside environment and polarization changes during the transfer of charges.[33] Since we are unable to rely on external RE to validate our estimates, we must restrict our attention to internal RE for the duration of this study. We have determined the RE for the mobility of both holes (λ_+) and electrons (λ_-) by using eqs 1 and 2[18] provided.

$$\lambda_+ = [E_+^0 - E_0] + [E_0^+ - E_+] \quad (1)$$

$$\lambda_- = [E_-^0 - E_0] + [E_0^- - E_-] \quad (2)$$

E_0^- and E_0^+ are the energies of anion and cation computed from the neutral molecule's ground state optimization. The anion and cation energies, E_- and E_+, respectively, are calculated using optimized anion and cation molecules. E_+^0 and E_-^0 are the energies of the neutral molecules, which are determined by the use of optimized cation and anion structures. The energy of the neutrally optimized ground state of a molecule is denoted by E_0.[34]

3. RESULTS AND DISCUSSION

3.1. Geometrical Optimization. Molecular geometries have a major impact on the optoelectronic properties.[35] It is shown in Figure S1 that the best-fitting DFT functional was used to optimize both the reference (**IT-SMR**) and the newly developed compounds (**IT-SM1** to **IT-SM6**). As a result of the molecules' extensive conjugation, which spans the whole molecule from core to extremities, charge may be transferred efficiently demonstrating that the delocalization of pi electrons makes charge transfer in these systems very strong. **IT-SMR** and **IT-SM1** to **IT-SM6** molecules were analyzed for their amount of planarity and conjugation by determining their dihedral angles ($\theta°$) and bond length (L_b) given in Table S1. The distance between two carbon atoms in a double bond (C═C) is 1.34 Å,

https://doi.org/10.1021/acsomega.2c07975
ACS Omega 2023, 8, 21425−21437

whereas the distance between two carbon atoms in a single bond (C−C) is 1.54 Å. Having an L_b between 1.41 and 1.42 Å, as shown in all of the compounds studied (**IT-SMR** and **IT-SM1** to **IT-SM6**), shows improved charge transmission characteristics as well as enables the conjugation facilitated delocalization of π-electrons. All compounds studied had θ° values between 0.0144 and 0.2900. It can be deduced that every molecule has a planar shape, and the EGs are in plane with the core of the molecule. Though the overall symmetry between the acceptor and donor of the molecules is quite planar, the four methoxy phenyl chains attached to the central IDTT donor do have a perpendicular orientation with respect to the rest of the plane of the molecule.

3.2. Study of Frontier Molecular Orbitals (FMOs). Examining the FMOs is crucial research because it reveals how effective molecules are in facilitating charge mobility and electron density dispersal.[36] It helps us figure out how the charge is transmitted and facilitated across OSCs. Molecules' HOMO and LUMO energy profoundly affect their charge transfer, light absorption, and electrical properties.[37] The energy gap (E_{gap}) is characteristic of OSCs and other photovoltaic systems; it represents the amount of energy required for the dissociation of electrons.[38] The efficiency of OSCs improves as their band gap (E_{gap}) reduces. To create reliable photovoltaic cells, compounds with the smallest feasible E_{gap} must be used. Molecules having a narrow E_{gap} are highly polarizable, kinetically unstable, and chemically reactive.[39] Table 1 displays estimated values for the

Table 1. HOMO, LUMO E_{gap}, IP, and EA of IT-SMR and IT-SM1 to IT-SM6

molecules	HOMO (eV)	LUMO (eV)	E_{gap}	IP (eV)	EA (eV)
IT-SMR	−5.42	−3.37	2.05	6.19	2.39
IT-SM1	−5.62	−3.54	2.07	6.40	2.76
IT-SM2	−5.97	−4.02	1.95	6.73	3.27
IT-SM3	−5.58	−3.54	2.04	6.21	2.79
IT-SM4	−5.45	−3.41	2.04	6.21	2.67
IT-SM5	−5.56	−3.53	2.02	6.31	2.80
IT-SM6	−5.51	−3.43	2.07	6.17	2.70

HOMO, LUMO, and E_{gap} energies of the **IT-SMR** and **IT-SM1** to **IT-SM6** molecules, which are used to assess the impact of different EG acceptors on the photophysical properties of the considered molecules.

Each molecule's HOMO and LUMO, together with their respective E_{gap}, are shown in Figure S2. The ground state of a molecule has most of its charge concentrated in its central area, known as the donor region. When molecules are in their excited state, the charges transfer to the outermost regions of the molecule, known as the EG acceptor regions. The charge mobility aspects of molecules from donor to acceptor sites is the evidence of the efficient conjugation that makes it possible for impactful charge transport functionalities as a result of the planar geometries of molecular. The HOMO and LUMO energy of the **IT-SMR** molecule were −5.43 and −3.33 eV, respectively, while its E_{gap} was 2.05 eV. The HOMO value of the **IT-SM2** molecule was the lowest (−5.97 eV), suggesting that it possessed the most stable HOMO of all of the molecules evaluated. Pairs of the electronegative cyano group in the periphery EG units of the IT-SM2 molecule have likely contributed significantly to the charge density dispersion, making its ground state more stable. As a result of its relatively low HOMO energy of −5.62 eV, **IT-SM1** is the second-most stable HOMO after **IT-SM2**. The **IT-SM1** molecule is more stable because of the presence of cyano and fluoro groups in its EGs. Energy levels of the HOMO and LUMO orbitals for the investigated compounds show diminishing patterns, i.e., **IT-SMR** > **IT-SM4** > **IT-SM6** > **IT-SM5** > **IT-SM3** > **IT-SM1** > **IT-SM2** and **IT-SMR** > **IT-SMIT-SM4** > **IT-SM6** > **IT-SM5** > **IT-SM3** = **IT-SM1** > **IT-SM2**, respectively. **IT-SM2** to **IT-SM5** molecules have smaller E_{gap} than the **IT-SMR** molecule. The E_{gap} is reduced as a consequence of the powerful electron-withdrawing EGs, which aids in charge transfer capabilities of the molecule. **IT-SM6** = **IT-SM1** > **IT-SMR** > **IT-SM5** > **IT-SM3** = **IT-SM4** > **IT-SM2** is the decreasing trend in E_{gap} for all.

3.3. Ionization Potential (IP) and Electron Affinity (EA). Effective charge transfers can be affected by a variety of factors, such as IP and EA. The energy output from adding electrons to the molecule is EA, while the required energy to remove the electron is IP.[40] Higher IP and EA values indicate that a molecule has a higher stable HOMO energy, hindering the process of electron removal; molecules with small IPs and EAs are capable of effectively releasing electrons. Compounds with high IP and EA are caused by electron-withdrawing units that stabilize the HOMO, whereas molecules having small IP and EA are caused by electron donor units that destabilize the HOMO.[41] IP and EA are determined by using eqs 3 and 4.

$$\mathrm{IP} = [E_0^+ - E_0] \tag{3}$$

$$\mathrm{EA} = [E_0 - E_0^-] \tag{4}$$

Computationally estimated IP and EA values of compounds **IT-SMR** and IT-SM1 to **IT-SM6** can be found in Table 1. **IT-SMR** with the highest HOMO destabilization (−5.42 eV) has the least IP (6.19 eV) and EA (2.39 eV). The HOMO (−5.97 eV) of **IT-SM2** is the most stable, it has the greatest IP (6.73 eV) and EA (3.27 eV). **IT-SM1** possesses the second-greatest IP (6.40 eV) because it exhibits the second-highest stable HOMO (−5.62 eV). Among the new theoretically developed molecules, **IT-SM4** has the highest HOMO (−5.45 eV) and hence exhibits the smallest EA (2.67 eV).

3.4. Light Absorption Properties. By analyzing the optical absorbance spectrum, we can infer the chromophore's electrical specifications with high accuracy.[23a] Tables 2 and 3 show the

Table 2. Computed λ_{max}, E_x, Oscillator Strength (f), Assignment, and Dipole Moment (D) of IT-SMR and IT-SM1 to IT-SM6 Compounds in the Gas Phase

molecules	computed λ_{max} (nm)	E_x (eV)	f	assignment	D
IT-SMR	670	1.84	2.41	H → L (99%)	3.31
IT-SM1	663	1.87	2.32	H → L (99%)	3.33
IT-SM2	708	1.75	2.07	H → L (98%)	3.44
IT-SM3	677	1.83	2.37	H → L (99%)	3.29
IT-SM4	675	1.83	2.63	H → L (99%)	3.22
IT-SM5	682	1.81	2.62	H → L (99%)	3.34
IT-SM6	669	1.85	2.70	H → L (99%)	3.30

approximated results for the gaseous and solvent (chloroform) phases, respectively, from a spectrum assessment of **IT-SMR** and **IT-SM1** to **IT-SM6** molecules using the above-mentioned level of theory, i.e., B3LYP/6-31G(d,p). Figure 3 displays the absorption spectra for **IT-SMR** and **IT-SM1** to **IT-SM6** from 450 to 1250 nm in the gas phase and from 450 to 1400 nm in the chloroform ($CHCl_3$) solvent. **IT-SMR** has a gas-phase λ_{max} of 670 nm and a solvent-phase λ_{max} of 709 nm. The λ_{max} of **IT-SM2**

https://doi.org/10.1021/acsomega.2c07975
ACS Omega 2023, 8, 21425−21437

Table 3. Computed λ_{max}, E_x, Oscillator Strength (f), Assignment, and Dipole Moment (D) of IT-SMR and IT-SM1 to IT-SM6 Compounds in $CHCl_3$

molecules	exp. λ_{max} (nm)	computed λ_{max} (nm)	E_x (eV)	f	assignment	D
IT-SMR	~691	709	1.74	2.84	H → L (98%)	3.96
IT-SM1		704	1.76	2.71	H → L (98%)	3.98
IT-SM2		758	1.63	2.45	H → L (98%)	4.12
IT-SM3		723	1.71	2.70	H → L (98%)	3.95
IT-SM4		715	1.73	3.04	H → L (98%)	3.86
IT-SM5		722	1.71	3.02	H → L (98%)	4.00
IT-SM6		707	1.75	3.07	H → L (98%)	3.94

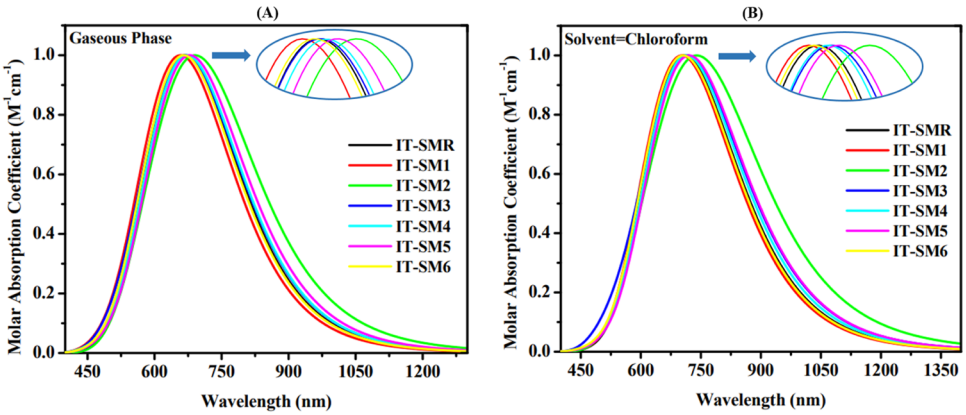

Figure 3. Absorbance spectrum of **IT-SMR** and **IT-SM1** to **IT-SM6** molecules in (A) the gas phase and (B) the $CHCl_3$ solvent.

to **IT-SM6** molecules is redshifted from **IT-SMR** from 675 to 708 nm in the gas phase and from 715 to 758 nm in the $CHCl_3$ solvent. **IT-SM2** to **IT-SM6** compounds demonstrated a bathochromic in their λ_{max} relative to the **IT-SMR** in the UV−visible spectrum, with a shift of 5−38 nm and a shift of 6−49 nm, in both examined phases, respectively. The planar structure of the molecules allows for more effective conjugation, leading to enhanced optical absorption. Based on the basic concept that the solvent that is polar stabilizes the polar excited state, the studied molecules revealed a bathochromic transition in the $CHCl_3$ solvent as compared to the gas form.[42] The wavelength and energy are inversely related to each other, so all of the molecules with the shortest E_{gap} also had the longest wavelength. **IT-SM1 < IT-SM6 < IT-SMR < IT-SM4 < IT-SM3 < IT-SM5 < IT-SM2** and **IT-SM1 < IT-SM6 < IT-SMR < IT-SM4 < IT-SM5 < IT-SM3 < IT-SM2** is the increasing λ_{max} trend of the studied compounds in the gas phase and in the $CHCl_3$ solvent, respectively. The results show that IT-SM2, at 708 and 758 nm, has the greatest λ_{max} in both phases (gas and solvent), respectively. It might be because the EG acceptors contain a couple of electronegative cyano groups.

Both the optical features of OSC devices and the radiation intensity generated by electrical excitation across the energy levels are significantly reliant on a variable that has no dimensions and is referred to as the oscillator strength (f).[43] Excitation energy (E_x) is a kind of energy which is required in order to accomplish a probable shift.[44] In reality, raising the f, decreasing the E_x, or expanding the absorption spectrum may all improve ICT's performance. Compared to **IT-SMR**, **IT-SM2** to **IT-SM5** compounds have a bigger f whereas **IT-SM4** to **IT-SM5** compounds have a broader absorption range and a smaller E_x; this might lead to improved ICT aspect in the compound.

3.5. Dipole Moment (*D*). The dipole moment (D) plays an important part in the process of defining the crystalline nature and solubility. In the solvent required for effective OSC systems, these features play a significant role in determining polarizing activities.[45] The planar and organized morphology of compounds with a significant D value makes it possible for the charge to be transferred in a consistent manner. This, in turn, leads to tight structural packing, which improves the crystalline nature and results in greater solubility in polar solvents. Molecules having a greater D likely become more crystalline, and they diffuse more readily in polar solvents as a result, both of which improve charge conduction.[46] Polar organic solvents like $CHCl_3$ tend to be insoluble for molecules lacking a dipole moment. Overall, the relationship between them is not fundamental since each molecule has a unique chemical morphology that determines its charge transfer and solubility characteristics.[47] According to the numerical data shown in Tables 3 and 4, the

Table 4. Oscillator Strength and LHE of IT-SMR and IT-SM1 to IT-SM6 Molecules

molecules	f	LHE
IT-SMR	2.84	0.9985
IT-SM1	2.71	0.9981
IT-SM2	2.45	0.9964
IT-SM3	2.70	0.9980
IT-SM4	3.04	0.9991
IT-SM5	3.02	0.9990
IT-SM6	3.07	0.9991

ascending order of D for the compounds was investigated in both phases (gas and $CHCl_3$, respectively), i.e., **IT-SM4 < IT-SM3 < IT-SM6 < IT-SMR < IT-SM1 < IT-S5 < IT-SM2** and **IT-SM4 < IT-SM6 < IT-SM3 < IT-SMR < IT-SM1 < IT-S5 < IT-SM2**. Solubility as well as crystallinity of **IT-SM1**, **IT-SM2, and IT-SM5** are much better than those of **IT-SMR** owing to the higher D values of these molecules. **IT-SM2** had the greatest

https://doi.org/10.1021/acsomega.2c07975
ACS Omega 2023, 8, 21425−21437

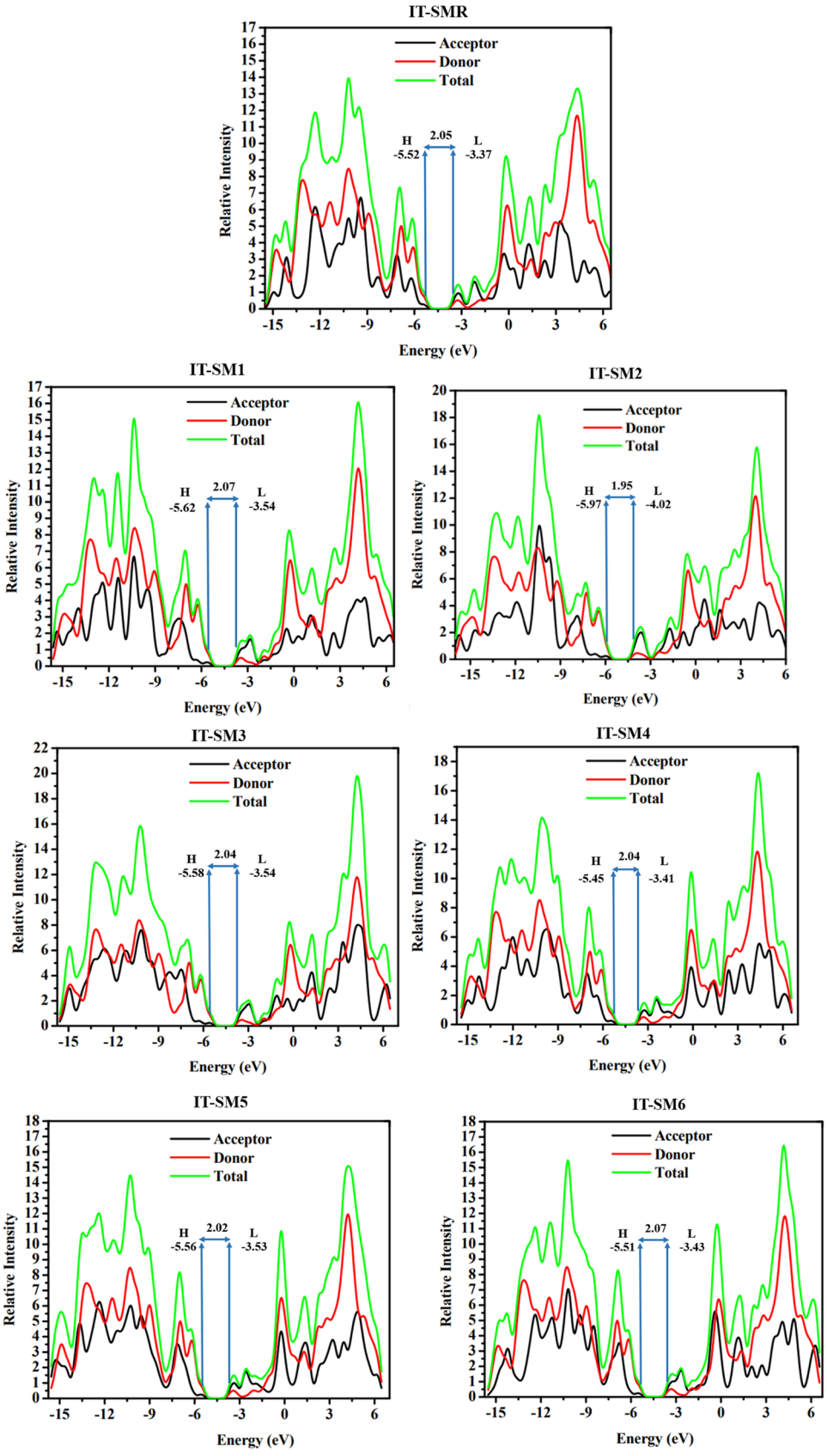

Figure 4. DOS graphs of **IT-SMR** and **IT-SM1** to **IT-SM6** molecules.

D value, which may be explained by the occurrence of cyano groups at the EGs.

3.6. Light-Harvesting Efficiency (LHE). Every solar cell's element has to be capable of producing a charge after light absorbance, generally known as LHE.[48] The absorption

https://doi.org/10.1021/acsomega.2c07975
ACS Omega 2023, 8, 21425−21437

performance of the system is affected by LHE, which is in turn influenced by the oscillator strength due to its effect on the amount of short-circuit current (J_{SC}) it generates. The LHE for every compound studied was determined with the use of eq 5.[38]

$$\mathrm{LHE} = 1 - 10^{-f} \quad (5)$$

The LHE values calculated for **IT-SMR** and **IT-SM1** to **IT-SM6** molecules in chloroform are enlisted in Table 4. Compared to IT-**SMR**, the LHE value of **IT-SM4**, **IT-SM5**, and **IT-SM6** molecules were all higher. **IT-SM6** has greater oscillation strength, which results in the greatest LHE. In line with the results, the LHE of **IT-SM4**, **IT-SM5**, and **IT-SM6** molecules is profoundly influenced by the EG acceptors.

3.7. Density of States (DOS). DOS studies are crucial for developing a comprehensive understanding of the roles played by the constituent parts (e.g., donor and acceptor) of any given compound. The full potential of molecules is determined by the DOS that corresponds to them, which may either be partial or complete.[49] The determination of DOS is an essential step in determining the layout of FMOs in relation to the Mulliken charge distribution.[50] The DOS for each of the molecules that were investigated was computed at the B3LYP/6-31G(d,p) level of theory, as well as charts of the readings were produced using the PyMOlyze 1.1 program. DOS plots provide a graphical representation of both the energies, which is displayed along the *x*-axis, and the relative intensity, which is shown along the *y*-axis. In the graphs, the peaks that represent the HOMO energy are located to the left of the central plane (the E_{gap}), while the peaks that indicate the LUMO energy are located to the right of the central plane. To examine the contribution of every unit to the FMOs, we split each molecule into two parts, identifying the donor and acceptor units.

The acceptor and donor involvement is denoted by black and red lines, respectively, in the DOS plots of **IT-SMR** and **IT-SM1** to **IT-SM6**, whereas a green line represents the total contribution that the moieties made to the creation of the FMO, as depicted in Figure 4, and the numerical estimations of the contributions by different subunits are given in Table 5. Here, in Figure 6, it can be seen that the PDOS in the case of the donor is the same in all of the studied molecules; however, the PDOS of acceptors (black peaks) changes significantly in all of the molecules. Here, it can be seen that just because of the varying acceptor peaks, the intensity of TDOS is also varying significantly, with that of IT-SMR being the lowest one among all. This intense peak on the right side of the graphs, i.e., the conduction band, illustrates the greater probability of charge separation in the designed molecules. From the analysis of data, it is estimated that all studied compounds show almost the same pattern of contribution of molecular subunits in the FMOs, i.e., the central donor subunit demonstrating dominating role in the HOMO state and the acceptor part playing a larger role in the LUMO state. This conclusively proves that charge may easily move from the donor to acceptor components of a compound by sequential conjugation that has the potential to boost the OSCs' overall efficiency. These results are consistent with the FMOs of the molecules that were studied, as shown in Figure 4. These findings indicate that the donor core region of the molecule, which is abundant in electrons, predominates in the ground state of the molecule and charge is being transferred efficiently from the donor core area to the electron-accepting EGs in the excited state of molecules because of the planar structure of molecules.

Table 5. Acceptor and Donor Subunits Involvement in the FMOs of Investigated Molecules

molecules		acceptor (%)	donor (%)
IT-SMR	HOMO	26.9	73.1
	LUMO	60.8	39.2
IT-SM1	HOMO	24.4	75.6
	LUMO	61.1	38.9
IT-SM2	HOMO	25.4	74.6
	LUMO	66.3	33.7
IT-SM3	HOMO	25.0	75.0
	LUMO	63.1	36.9
IT-SM4	HOMO	26.2	73.8
	LUMO	61.1	38.2
IT-SM5	HOMO	26.2	73.8
	LUMO	62.3	37.7
IT-SM6	HOMO	25.4	74.6
	LUMO	60.4	39.6

3.8. Analysis of Charge Mobility. In order to explore the charge mobility from the acceptor to donor components, the reorganization energy (RE) of **IT-SM1** to **IT-SM6** and **IT-SMR** molecules was evaluated at B3LYP functional. The RE is the most important component in the design of efficient substances for OSCs because it provides a quantitative measure of the charge transferred from the donor portion to the acceptor parts of a molecule and is therefore related to the electron and hole mobility of the molecule.[51] In fact, the RE has an adverse correlation with the mobility of holes and electrons. As a consequence of this, decreasing the RE will lead to a charge conveyance that is more efficient.[52] The geometric configurations of anion and cation are only one of the numerous variables that might have an effect on the RE. Using eqs 1 and 2, the electron and hole RE values for each of the compounds under investigation are determined, and the results are presented in Table S2 and Figure 5, respectively. According to the results, the greater hole and electron mobility reported in some of the recently proposed molecules are likely the result of a better molecular mix owing to their planar geometries.

The **IT-SMR** molecule has a RE of 0.1605 eV for the λ_- and 0.1702 eV for the λ_+. With lesser RE of λ_-, **IT-SM2**, **IT-SM3**, and **IT-SM5** have improved electron mobility than **IT-SMR**. The fine morphology of the resultant molecule blend is due to the planar molecular geometries, which enhance the dissociation of exciton as well as the electron mobility. Since it was determined that the RE of **IT-SM2** for electron mobility was the lowest (0.1127 eV) of all of the molecules that were investigated, this leads one to believe that the molecule's newly added EGs have had a substantial role in the enhancement of its electron transport capabilities. The sequence of λ_- for the compounds that were investigated is **IT-SM2** < **IT-SM5** < **IT-SM3** < **IT-SMR** < **IT-SM4** = **IT-S6** < **IT-SM1**. Because the RE of **IT-SM6** (0.0907 eV) for hole mobility has reduced astonishingly, it has the highest hole mobility of any of the molecules that have been tested. The dramatic decrease in the hole's RE for the IT-SM6 molecule suggests that the bromo-functionalized thiophene containing EG is considerably participating in the reduction of the RE to increase hole mobility.

3.9. Electrostatic Potential (ESP). The presence of electrons and the 3D dispersion of charge outside of a molecule are brought to the fore by ESP.[53] The ESP method was used for the compounds that we meticulously researched in order to make predictions about the reactive sites included inside a

https://doi.org/10.1021/acsomega.2c07975
ACS Omega 2023, 8, 21425−21437

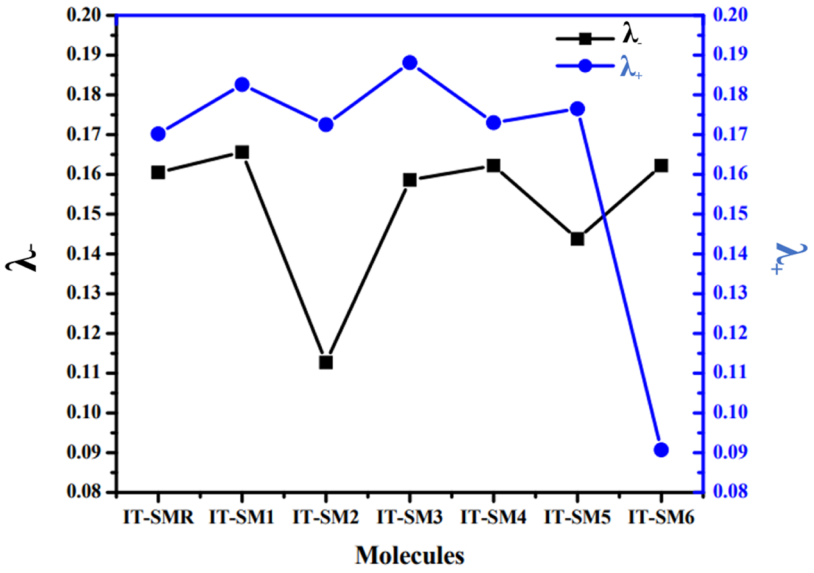

Figure 5. RE graphs of **IT-SMR** and **IT-SM1** to **IT-SM6** molecules for the electron and hole mobility.

molecule's structure. On the ESP maps, the 3D arrangement of electron pairs, free electrons, and electronegative components that may easily be subjected to nucleophilic reaction is shown. On the ESP modeling, the color red represents an area that has a higher electron density, green represents an area that is neutral, and blue represents an area that has a lower electron density. Concentrations of electrons over oxygen and nitrogen atoms at the EGs of molecules appear as dark red blotches on ESP diagrams (Figure S3). It is concluded that the existence of oxygen at the EGs revealing the red color indicates the electron density over these sites; on the other hand, the existence of oxygen in the core of molecules depicting blue and green colors is because the electron-poor carbon atoms in the vicinity cancel out the oxygen's electrical density in the core region.[54] The benzene and thiophene rings, as well as methyl groups that act as donors are colored blue on the ESP maps, suggesting a severe lack of electrons there.

3.10. Transition Density Matrix (TDM). TDM evaluation is crucial to accurately predict the exciton flow between the acceptor and donor units at specified locations in conjugated molecular structures.[55] Using this method, it is possible to anticipate charge transmission, principal charge spots, and the location of exciton movements during emissions and absorption in the excited state.[56] TDM plots are often produced for the purpose of analyzing electronic properties, such as the resonating impact and level of delocalization, and to learn about the movement of charges within a molecule. In TDM studies, the contribution of hydrogen is frequently ignored since its effect on charge transfer is considered to be insignificant. The *y*-axis on the left and the *x*-axis on the bottom represent the total number of atoms in molecules besides hydrogen. The electrostatic potential coefficient is shown by the column on the right side of the graph that has a number of different colors on it and goes from blue to red as it moves down the *x*-axis. Figure 6 shows that the electrical density exists in both acceptor (A) and donor (D) regions of every molecule we examined (**IT-SMR** and **IT-SM1** to **IT-SM6**). Both a diagonal and an off-diagonal pattern are followed by the consistent flow of electrostatic potential as it moves to the acceptor from the donor throughout the compound, with the diagonal pattern being the more common of the two. The illustration revealed the orderly transfer of electrical density from the donor core section to the EGs of the compounds through consecutive conjugation, which provided evidence for efficient charge distribution. The interaction coefficient (IC) for each of the compounds that were investigated was calculated and is shown in Table 6. Additionally, the escalating pattern of the IC is **IT-SM6** < **IT-SM4** < **IT-SM5** < **IT-SMR** < **IT-SM3** < **IT-S2** < **IT-SM1**. The fact that the IC of **IT-SM6** is low suggests that it is very simple for electrons to move between the acceptor and donor regions of this compound. This is because a smaller molecule's IC is expected to result in enhanced charge mobility.

3.11. Exciton Binding Energy (E_b). Another crucial factor is E_b, which may be used to gauge the possibility of exciton (electron−hole) segregation, OSCs' functionality in addition to their electrical properties.[57] The value of E_b is the result of calculating the interactions based on Coulombic forces that occur between electron−hole pairs.[58] If E_b is low, then the Coulombic interaction between electrons and holes is weak, and vice versa. Table 6 displays the predicted values for E_b based on eq 6 from this analysis.

$$E_b = E_{gap} - E_x \quad (6)$$

In the gas phase, the **IT-SM1** and **IT-SM2** molecules have a lower E_b value (at 0.20 eV) than the **IT-SMR** molecule, as shown by the computed values. Comparing the E_b values of **IT-SM3**, **IT-SM4**, and **IT-SM5** to those of **IT-SMR**, we find that they are almost identical. In the $CHCl_3$ solvent, the E_b of **IT-SM4** (0.29 eV) has the lowest value. These compounds are promising options for greater charge potential because of exciton diffusion into free charges due to their low E_b value. Additionally, the slightly higher value of the binding energy in the **IT-SM6** molecule could be attributed to its greater interactive properties and higher band gap values, and thus it might not be the best molecule so far.

The interaction coefficient is another important parameter, which, just like the binding energy, is the lower the better. It actually regulates the possibility of charge separation and determines the degree of interaction between the charges. Molecules with greater charge separation would have a lower interaction coefficient.[59] The interaction coefficient (IC) of the studied molecules follows the descending order **IT-SM1** > **IT-**

https://doi.org/10.1021/acsomega.2c07975
ACS Omega 2023, 8, 21425−21437

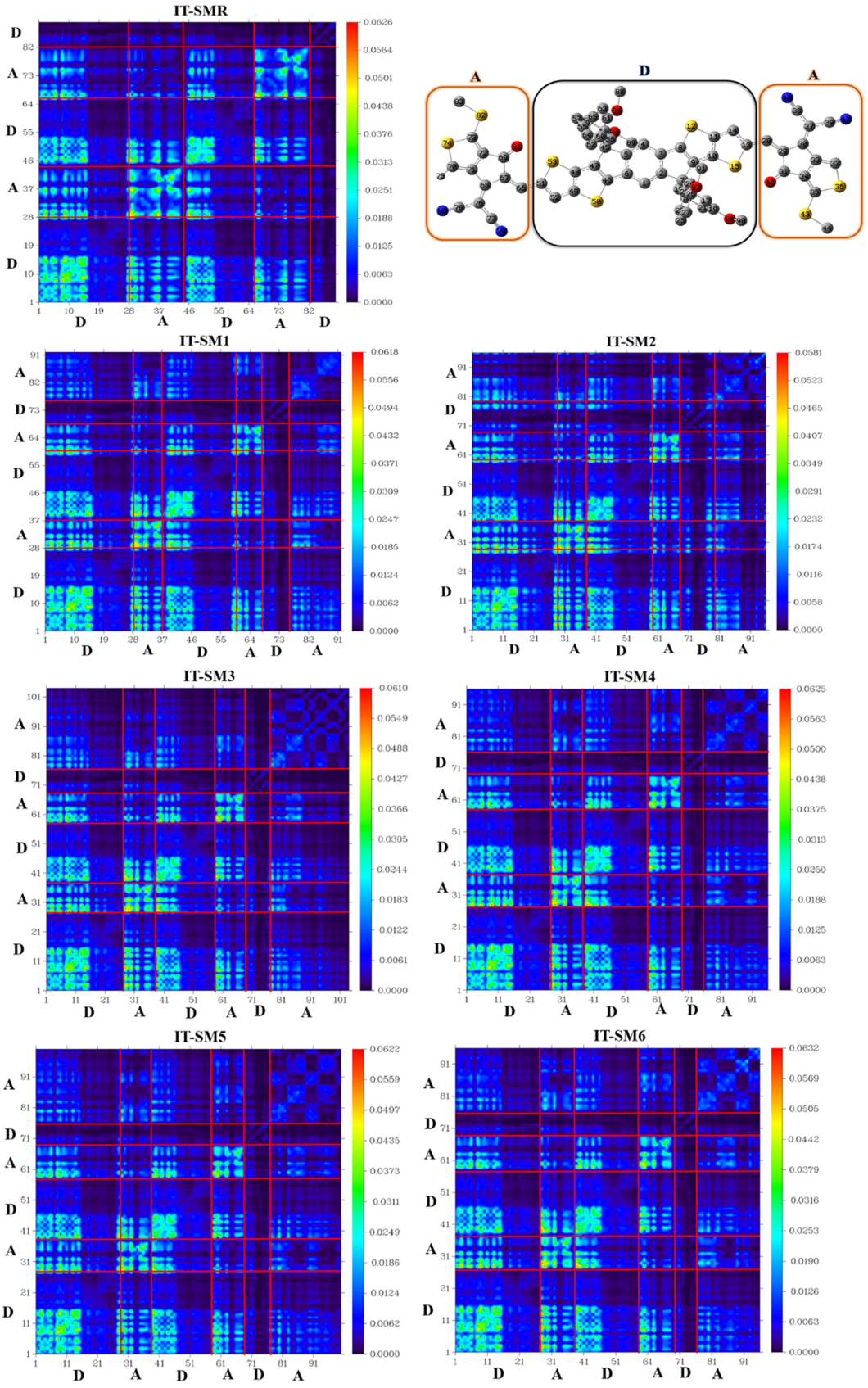

Figure 6. TDM plots of **IT-SMR** and **IT-SM1** to **IT-SM6** molecules.

SM2 > **IT-SM3** > **IT-SMR** > **IT-SM5** > **IT-SM4** > **IT-SM6**. This shows that the IC value of **IT-SM6** is the lowest, which illustrates its better transfer of charges.

3.12. Device Performance. In order to evaluate the efficiency of an OSC, it is necessary to measure the device's open-circuit voltage (V_{OC}).[60] The value of V_{OC} is an accurate

https://doi.org/10.1021/acsomega.2c07975
ACS Omega 2023, 8, 21425−21437

Table 6. E_{gap}, E_b (Gas Phase and $CHCl_3$ Solvent), and the Interaction Coefficient of the Studied Molecules

molecules	E_{gap} (eV)	E_b (eV) (gas)	E_b (eV) ($CHCl_3$)	IC
IT-SMR	2.05	0.21	0.31	0.70141
IT-SM1	2.07	0.20	0.31	0.70169
IT-SM2	1.95	0.20	0.32	0.70166
IT-SM3	2.04	0.21	0.33	0.70150
IT-SM4	2.04	0.21	0.29	0.70102
IT-SM5	2.02	0.21	0.31	0.70120
IT-SM6	2.07	0.22	0.32	0.70078

reflection of the greatest voltage that a solar device is capable of producing when the input voltage is zero. Light intensity, charge transfer, photovoltaic device temperature, etc., all play crucial roles in V_{OC}.[61] When the HOMO of the donor substance and the LUMO of the acceptor substance are coupled with one another, the maximum voltage is produced. In order to obtain the enhanced V_{OC} values, the HOMO energy state of the donor must be smaller, and the LUMO energy state of the acceptor must be higher. In the current investigation, the V_{OC} of theoretically constructed donor molecules (**IT-SMR** and **IT-SM1** to **IT-SM6**) was calculated by associating those molecules with a $PC_{61}BM$ acceptor (Table 7). In accordance with the

Table 7. V_{OC}, Normalized V_{OC}, and FF of IT-SMR and IT-SM1 to IT-SM6 Molecules

molecules	V_{OC} (eV)	normalized V_{OC}	FF
IT-SMR	1.42	54.92	0.9102
IT-SM1	1.62	62.66	0.9191
IT-SM2	1.97	76.20	0.9307
IT-SM3	1.58	61.11	0.9175
IT-SM4	1.45	56.08	0.9117
IT-SM5	1.56	60.34	0.9166
IT-SM6	1.51	58.40	0.9145

available data, $PC_{61}BM$ is a reliable acceptor with HOMO and LUMO energies of −6.10 and −3.70 eV, respectively.[62] In this study, we employed eq 7 to produce a numerical estimate of V_{OC} concentrations.

$$V_{OC} = \frac{E_{ACCEPTOR}^{LUMO} - E_{DONOR}^{HOMO}}{e} - 0.3 \quad (7)$$

The molecule charge is represented by the character e, which is 1, and an intersurface charge factor, which typically has the value of 0.30 in the equation above. Figure 7 depicts the estimated V_{OC} together with the HOMO and LUMO energy levels of the proposed donor molecules and the $PC_{61}BM$ acceptor. According to the findings, it can be deduced that molecules **IT-SM1** to **IT-SM6** have higher V_{OC} values, which range from 1.45 to 1.97 eV, in comparison with the V_{OC} of **IT-SMR** (1.42 eV). **IT-SMR < IT-SM4 < IT-SM6 < IT-SM5 < IT-SM3 < IT-SM1 < IT-SM2** is the elevating sequence of V_{OC} of all studied compounds. In this research, the **IT-SM2** was found to exhibit the highest V_{OC} value, indicating that it has the ability to be used in increasing the PCE of OSC.

Among the most critical aspects in calculating an organic photovoltaic system's PCE is the fill factor (FF) because they are intimately tied to one another. FF is significantly influenced by the V_{OC} at the contact between the acceptor and donor components. All of the compounds in our study had their FFs calculated using eq 8.

$$FF = \frac{\frac{eV_{OC}}{K_B T} - \ln\left(\frac{eV_{OC}}{K_B T} + 0.72\right)}{\frac{eV_{OC}}{K_B T} + 1} \quad (8)$$

In this context, $\frac{eV_{OC}}{K_B T}$ is referred to as the normalized V_{OC}, where e is the standard charge, which is always equal to 1. K_B is the Boltzmann constant with the value of $8.61733034 \times 10^{-5}$ eV/K and T is the temperature, i.e., 300 K. The normalized V_{OC} is the V_{OC} value taking the necessary conditions of charge and temperature into account.[63] As per the concluded results, the newly proposed molecules have better normalized V_{OC} and FF (56.08−76.20 and 0.9117−0.9307) as compared to the parent molecule (54.92 and 0.9102), respectively (Table 7).

To ascertain whether or not the solar material is efficient enough for use in operative deployments, power conversion efficiency (PCE) is estimated, which summarizes all operational variables of solar devices into a single figure.[64] The V_{OC}, FF, and J_{SC} all have direct effects on a molecule's PCE. Equation 9[54] provides a good depiction of this relationship.

$$PCE = \frac{J_{SC}\, V_{OC}\, FF}{P_{in}} \quad (9)$$

In this work, we computationally calculate the V_{OC} and FF for the molecules **IT-SMR** and **IT-SM1** to **IT-SM6** using the preceding equations; the J_{SC}, though, was not calculated due to the insufficient facilities involved. LHE is among the factors used to estimate the J_{SC}, and it has been discussed in detail above. All recently developed compounds in this research exhibit greater PCE than **IT-SMR**, as predicted, due to their higher V_{OC} and FF.

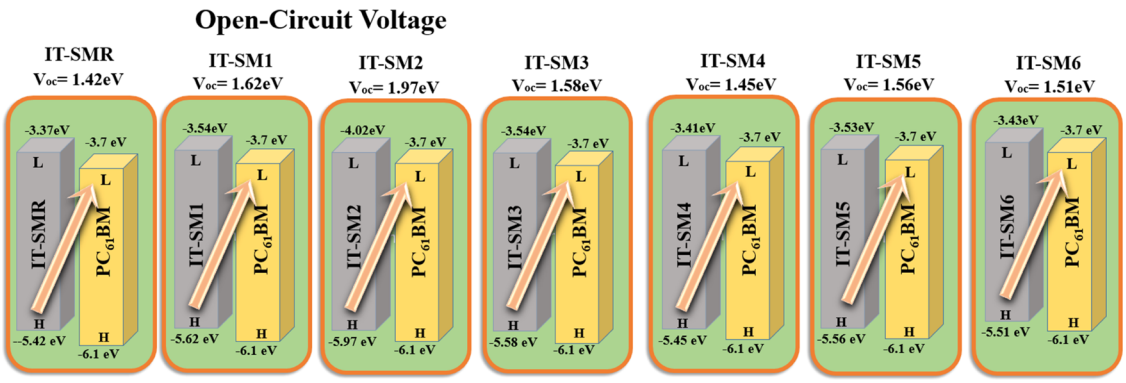

Figure 7. V_{OC} of **IT-SMR** and **IT-SM1** to **IT-SM6** donor molecules with $PC_{61}BM$.

https://doi.org/10.1021/acsomega.2c07975
ACS Omega 2023, 8, 21425−21437

These non-fullerene donors have been shown to have excellent optoelectronic features, and the theoretical estimates show that they may be applicable in practical operation.

4. CONCLUSIONS

In the current research, six 3D small donor molecules (**IT-SM1** to **IT-SM6**) have been computationally created to improve the performance of OSCs by altering the EG acceptor of the reference molecule (**IT-SMR**). Using the B3LYP/6-31G(d,p) level of theory, we calculate several optoelectronic characteristics of the newly developed compounds and compare them to the parent molecule. **IT-SM2** to **IT-SM5** molecules have smaller E_{gap} (range of 2.04−1.95 eV) and bathochromic shift in their λ_{max} (range of 715−758 nm) as compared to the **IT-SMR** molecule (2.05 eV and 709 nm, respectively). When compared to other molecules, **IT-SM2** has the shortest E_{gap} (1.95 eV), smallest E_x (1.63 eV), largest λ_{max} (758 nm), and highest dipole moment (4.12 D). **IT-SM6** has the lowest IP (6.17 eV), while **IT-SM2** has the highest EA (3.27 eV). Compared to IT-**SMR**, the LHE value of **IT-SM4**, **IT-SM5**, and **IT-SM6** molecules were all higher. Because of having a lower RE of λ_-, **IT-SM2**, **IT-SM3**, and **IT-SM5** (0.1127, 0.1586, and 0.1430 eV, respectively) exhibit higher electron mobility than **IT-SMR** (0.1605 eV). RE of **IT-SM2** for hole mobility was the lowest (0.1127 eV) of all of the molecules that were investigated. In the $CHCl_3$ solvent, the exciton binding energy of **IT-SM4** (0.29 eV) has the lowest value. The V_{OC} of the investigated donor molecules was evaluated by connecting them to the $PC_{61}BM$, and analysis revealed that all of the newly suggested molecules (**IT-SM1** to **IT-SM6**) had higher V_{OC} and fill factor (FF) values than the **IT-SMR** molecule. Based on the results of this study, the modified molecules may be investigated further for potential use in the production of organic solar cells with enhanced photovoltaic capabilities.

■ ASSOCIATED CONTENT

Supporting Information

The Supporting Information is available free of charge at https://pubs.acs.org/doi/10.1021/acsomega.2c07975.

Cartesian coordinates of all of the molecules of the study; optimized geometries; FMOs; ESP plots; computed L_b and dihedral angles ($\theta°$); and RE of electron (λ-) and hole (λ+) mobility (PDF)

■ AUTHOR INFORMATION

Corresponding Author

Amira K. Hajri − *Department of Chemistry, Alwajh College, University of Tabuk, Tabuk 47512, Saudi Arabia;* orcid.org/0000-0002-3530-1204; Email: ahejari@ut.edu.sa

Authors

Fahed A. Aloufi − *Department of Environment, Faculty of Environmental Sciences, King Abdulaziz University, Jeddah 21589, Saudi Arabia*

Riyadh F. Halawani − *Department of Environment, Faculty of Environmental Sciences, King Abdulaziz University, Jeddah 21589, Saudi Arabia;* orcid.org/0000-0001-8121-7524

Bassem Jamoussi − *Department of Environmental Science, Faculty of Meteorology, Environment and Arid Land Agriculture, King Abdulaziz University, Jeddah 21589, Saudi Arabia;* orcid.org/0000-0003-4520-4202

Nesrine Zahi − *Applied College, Huraymila, Imam Mohammad Ibn Saud Islamic University (IMSIU), Riyadh 11564, Saudi Arabia; Thermal and Energetic Systems Studies Laboratory (LESTE), National Engineering School of Monastir (ENIM), University of Monastir, Monastir 5000, Tunisia*

Complete contact information is available at: https://pubs.acs.org/10.1021/acsomega.2c07975

Funding

This research work was funded by the Institutional Fund Projects under Grant No. IFPIP:1241-155-1443.

Notes

The authors declare no competing financial interest.

■ ACKNOWLEDGMENTS

The authors gratefully acknowledge technical and financial support provided by the Ministry of Education and King Abdulaziz University, DSR, Jeddah, Saudi Arabia.

■ REFERENCES

(1) Mahalingavelar, P. How End-Capped Acceptors Regulate the Photovoltaic Performance of the Organic Solar Cells: A Detailed Density Functional Exploration of Their Impact on the A−D− π−D−A Type Small Molecular Electron Donors. *Energy Fuels* **2022**, *36*, 2095−2107.

(2) (a) Hu, Z.; Wang, J.; Ma, X.; Gao, J.; Xu, C.; Yang, K.; Wang, Z.; Zhang, J.; Zhang, F. A critical review on semitransparent organic solar cells. *Nano Energy* **2020**, *78*, No. 105376. (b) Paramasivam, M.; Gupta, A.; Raynor, A. M.; Bhosale, S. V.; Bhanuprakash, K.; Rao, V. J. Small band gap D-π-A-π-D benzothiadiazole derivatives with low-lying HOMO levels as potential donors for applications in organic photovoltaics: a combined experimental and theoretical investigation. *RSC Adv.* **2014**, *4*, 35318−35331.

(3) (a) Servaites, J. D.; Ratner, M. A.; Marks, T. J. Organic solar cells: A new look at traditional models. *Energy Environ. Sci.* **2011**, *4*, 4410−4422. (b) Wang, Y.; Lee, J.; Hou, X.; Labanti, C.; Yan, J.; Mazzolini, E.; Parhar, A.; Nelson, J.; Kim, J. S.; Li, Z. Recent progress and challenges toward highly stable nonfullerene acceptor-based organic solar cells. *Adv. Energy Mater.* **2021**, *11*, No. 2003002. (c) Li, J.; Sun, C.; Tang, A.; Zhang, B.; Guo, Q.; Zhou, E.; Li, Y. Utilizing an electron-deficient thieno [3, 4-c] pyrrole-4, 6-dione (TPD) unit as a π-bridge to improve the photovoltaic performance of A−π−D−π−A type acceptors. *J. Mater. Chem. C* **2020**, *8*, 15981−15984. (d) Ma, R.; Yang, T.; Xiao, Y.; Liu, T.; Zhang, G.; Luo, Z.; Li, G.; Lu, X.; Yan, H.; Tang, B. Air-processed efficient organic solar cells from aromatic hydrocarbon solvent without solvent additive or post-treatment: insights into solvent effect on morphology. *Energy Environ. Mater.* **2022**, *5*, 977−985. (e) Nie, Q.; Tang, A.; Guo, Q.; Zhou, E. Benzothiadiazole-based non-fullerene acceptors. *Nano Energy* **2021**, *87*, No. 106174.

(4) Cui, Y.; Xu, Y.; Yao, H.; Bi, P.; Hong, L.; Zhang, J.; Zu, Y.; Zhang, T.; Qin, J.; Ren, J.; et al. Single-junction organic photovoltaic cell with 19% efficiency. *Adv. Mater.* **2021**, *33*, No. 2102420.

(5) (a) Huang, Y.; Kramer, E. J.; Heeger, A. J.; Bazan, G. C. Bulk heterojunction solar cells: morphology and performance relationships. *Chem. Rev.* **2014**, *114*, 7006−7043. (b) Guo, Q.; Guo, Q.; Geng, Y.; Tang, A.; Zhang, M.; Du, M.; Sun, X.; Zhou, E. Recent advances in PM6: Y6-based organic solar cells. *Mater. Chem. Front.* **2021**, *5*, 3257−3280.

(6) (a) Reyes-Reyes, M.; Kim, K.; Dewald, J.; López-Sandoval, R.; Avadhanula, A.; Curran, S.; Carroll, D. L. Meso-structure formation for enhanced organic photovoltaic cells. *Org. Lett.* **2005**, *7*, 5749−5752. (b) Collins, B. A.; Tumbleston, J. R.; Ade, H. Miscibility, crystallinity, and phase development in P3HT/PCBM solar cells: toward an enlightened understanding of device morphology and stability. *J. Phys. Chem. Lett.* **2011**, *2*, 3135−3145. (c) Zhang, Y.; Ji, Y.; Zhang, Y.; Zhang, W.; Bai, H.; Du, M.; Wu, H.; Guo, Q.; Zhou, E. Recent Progress of Y6-

Derived Asymmetric Fused Ring Electron Acceptors. *Adv. Funct. Mater.* **2022**, *32*, No. 2205115.
(7) (a) Wang, H.; Cao, J.; Yu, J.; Zhang, Z.; Geng, R.; Yang, L.; Tang, W. Molecular engineering of central fused-ring cores of non-fullerene acceptors for high-efficiency organic solar cells. *J. Mater. Chem. A* **2019**, *7*, 4313−4333. (b) Nian, Y.; Wang, Z.; Jiang, H.; Feng, S.; Li, S.; Zhang, L.; Cao, Y.; Chen, J. Silaindacenodithiophene-Based Fused-Ring Non-Fullerene Electron Acceptor for Efficient Polymer Solar Cells. *Chin. J. Chem.* **2018**, *36*, 495−501. (c) Rashid, E. U.; Iqbal, J.; Khan, M. I.; El-Badry, Y. A.; Ayub, K.; Khera, R. A. Synergistic end-capped engineering on non-fused thiophene ring-based acceptors to enhance the photovoltaic properties of organic solar cells. *RSC Adv.* **2022**, *12*, 12321−12334.
(8) Xu, X.; Li, Z.; Bäcke, O.; Bini, K.; James, D. I.; Olsson, E.; Andersson, M. R.; Wang, E. Effects of side chain isomerism on the physical and photovoltaic properties of indacenodithieno [3, 2-b] thiophene−quinoxaline copolymers: toward a side chain design for enhanced photovoltaic performance. *J. Mater. Chem. A* **2014**, *2*, 18988−18997.
(9) (a) Li, F.; Tang, A.; Zhang, B.; Zhou, E. Indacenodithieno [3, 2-b] thiophene-based wide bandgap D-π-A copolymer for nonfullerene organic solar cells. *ACS Macro Lett.* **2019**, *8*, 1599−1604. (b) Murto, P.; Elmas, S.; Méndez-Romero, U. A.; Yin, Y.; Genene, Z.; Mone, M.; Andersson, G. G.; Andersson, M. R.; Wang, E. Highly Stable Indacenodithieno [3, 2-b] thiophene-Based Donor−Acceptor Copolymers for Hybrid Electrochromic and Energy Storage Applications. *Macromolecules* **2020**, *53*, 11106−11119.
(10) Lin, Y.; Wang, J.; Zhang, Z. G.; Bai, H.; Li, Y.; Zhu, D.; Zhan, X. An electron acceptor challenging fullerenes for efficient polymer solar cells. *Adv. Mater.* **2015**, *27*, 1170−1174.
(11) (a) Zhao, W.; Li, S.; Yao, H.; Zhang, S.; Zhang, Y.; Yang, B.; Hou, J. Molecular optimization enables over 13% efficiency in organic solar cells. *J. Am. Chem. Soc.* **2017**, *139*, 7148−7151. (b) Li, S.; Ye, L.; Zhao, W.; Zhang, S.; Mukherjee, S.; Ade, H.; Hou, J. Energy-level modulation of small-molecule electron acceptors to achieve over 12% efficiency in polymer solar cells. *Adv. Mater.* **2016**, *28*, 9423−9429. (c) Zhao, W.; Qian, D.; Zhang, S.; Li, S.; Inganäs, O.; Gao, F.; Hou, J. Fullerene-free polymer solar cells with over 11% efficiency and excellent thermal stability. *Adv. Mater.* **2016**, *28*, 4734−4739.
(12) (a) Han, C.; Wang, J.; Zhang, S.; Chen, L.; Bi, F.; Wang, J.; Yang, C.; Wang, P.; Li, Y.; Bao, X. Over 19% Efficiency Organic Solar Cells by Regulating Multidimensional Intermolecular Interactions. *Adv. Mater.* **2023**, *35*, No. 2208986. (b) Jeong, S.; Je, H.; Lee, J. H.; Lee, S. H.; Jang, S.-Y.; Park, K.; Kang, H.; Kwon, S.-K.; Kim, Y.-H.; Lee, K. Molecular engineering of non-fullerene acceptors based on thiophene-fused end groups for fullerene-free organic solar cells. *Dyes Pigm.* **2022**, *198*, No. 109987.
(13) Xie, D.; Liu, T.; Gao, W.; Zhong, C.; Huo, L.; Luo, Z.; Wu, K.; Xiong, W.; Liu, F.; Sun, Y.; Yang, C. A novel thiophene-fused ending group enabling an excellent small molecule acceptor for high-performance fullerene-free polymer solar cells with 11.8% efficiency. *Sol. RRL* **2017**, *1*, No. 1700044.
(14) Wang, P.; Bi, F.; Li, Y.; Han, C.; Zheng, N.; Zhang, S.; Wang, J.; Wu, Y.; Bao, X. Manipulating the intermolecular interactions through side chain engineering and unilateral π-bridge strategy for efficient small molecular photovoltaic acceptor. *Adv. Funct. Mater.* **2022**, *32*, No. 2200166.
(15) (a) Zhang, Z.; Feng, L.; Xu, S.; Yuan, J.; Zhang, Z.-G.; Peng, H.; Li, Y.; Zou, Y. Achieving over 10% efficiency in a new acceptor ITTC and its blends with hexafluoroquinoxaline based polymers. *J. Mater. Chem. A* **2017**, *5*, 11286−11293. (b) Luo, Z.; Li, G.; Gao, W.; Wu, K.; Zhang, Z.-G.; Qiu, B.; Bin, H.; Xue, L.; Liu, F.; Li, Y.; Yang, C. A universal nonfullerene electron acceptor matching with different bandgap polymer donors for high-performance polymer solar cells. *J. Mater. Chem. A* **2018**, *6*, 6874−6881. (c) Yan, C.; Wang, W.; Lau, T.-K.; Li, K.; Wang, J.; Liu, K.; Lu, X.; Zhan, X. Enhancing the performance of non-fullerene organic solar cells via end group engineering of fused-ring electron acceptors. *J. Mater. Chem. A* **2018**, *6*, 16638−16644.
(16) (a) Ye, L.; Zhang, S.; Zhao, W.; Yao, H.; Hou, J. Highly efficient 2D-conjugated benzodithiophene-based photovoltaic polymer with linear alkylthio side chain. *Chem. Mater.* **2014**, *26*, 3603−3605. (b) Cui, C.; Wong, W.-Y.; Li, Y. Improvement of open-circuit voltage and photovoltaic properties of 2D-conjugated polymers by alkylthio substitution. *Energy Environ. Sci.* **2014**, *7*, 2276−2284. (c) Patra, D.; Budiawan, W.; Huang, T.-Y.; Wei, K.-H.; Wang, P.-C.; Ho, K.-C.; Al-Hashimi, M.; Chu, C.-W. Enhanced organic solar cell performance by lateral side chain engineering on benzodithiophene-based small molecules. *ACS Appl. Energy Mater.* **2018**, *1*, 3684−3692.
(17) Zhao, B.; Wang, W.; Xin, J.; Wu, H.; Liu, H.; Guo, Z.; Cong, Z.; Ma, W.; Gao, C. Absorptive Behaviors and Photovoltaic Performance Enhancements of Alkoxy-Phenyl Modified Indacenodithieno [3, 2-b] thiophene-Based Nonfullerene Acceptors. *ACS Sustainable Chem. Eng.* **2018**, *6*, 2177−2187.
(18) Saeed, M. U.; Iqbal, J.; Mehmood, R. F.; Riaz, M.; Akram, S. J.; Somaily, H.; Shawky, A. M.; Raheel, M.; Khan, M. I.; Rashid, E. U.; Khera, R. A. Structural modification on Dimethoxythienothiophene based non-fullerene acceptor molecule for construction of high-performance organic chromophores by employing DFT approach. *J. Phys. Chem. Solids* **2022**, *170*, No. 110906.
(19) Frisch, M.; Trucks, G.; Schlegel, H.; Scuseria, G.; Robb, M.; Cheeseman, J.; Scalmani, G.; Barone, V.; Mennucci, B.; Petersson, G. *Gaussian 09*, revision D.01; Gaussian Inc.: Wallingford, CT, 2009.
(20) Dennington, R.; Keith, T. A.; Millam, J. M. *GaussView 6.0.16*; Semichem Inc.: Shawnee Mission, KS, 2016.
(21) Paramasivam, M.; Chitumalla, R. K.; Jang, J.; Youk, J. H. The impact of heteroatom substitution on cross-conjugation and its effect on the photovoltaic performance of DSSCs−a computational investigation of linear vs. cross-conjugated anchoring units. *Phys. Chem. Chem. Phys.* **2018**, *20*, 22660−22673.
(22) Paramasivam, M.; Kanvah, S. Rational tuning of AIEE active coumarin based α-cyanostilbenes toward far-red/NIR region using different π-spacer and acceptor units. *J. Phys. Chem. C* **2016**, *120*, 10757−10769.
(23) (a) Paramasivam, M.; Chitumalla, R. K.; Singh, S. P.; Islam, A.; Han, L.; Jayathirtha Rao, V.; Bhanuprakash, K. Tuning the photovoltaic performance of benzocarbazole-based sensitizers for dye-sensitized solar cells: a joint experimental and theoretical study of the influence of π-spacers. *J. Phys. Chem. C* **2015**, *119*, 17053−17064. (b) Civalleri, B.; Zicovich-Wilson, C. M.; Valenzano, L.; Ugliengo, P. B3LYP augmented with an empirical dispersion term (B3LYP-D*) as applied to molecular crystals. *CrystEngComm* **2008**, *10*, 405−410.
(24) Yanai, T.; Tew, D. P.; Handy, N. C. A new hybrid exchange−correlation functional using the Coulomb-attenuating method (CAM-B3LYP). *Chem. Phys. Lett.* **2004**, *393*, 51−57.
(25) Adamo, C.; Barone, V. Exchange functionals with improved long-range behavior and adiabatic connection methods without adjustable parameters: The m PW and m PW1PW models. *J. Chem. Phys.* **1998**, *108*, 664−675.
(26) Chai, J.-D.; Head-Gordon, M. Long-range corrected hybrid density functionals with damped atom−atom dispersion corrections. *Phys. Chem. Chem. Phys.* **2008**, *10*, 6615−6620.
(27) Tomasi, J.; Mennucci, B.; Cammi, R. Quantum mechanical continuum solvation models. *Chem. Rev.* **2005**, *105*, 2999−3094.
(28) Deschenes, L. A.; David, A.; Origin Lab Corporation (formerly Microcal Software, Inc.). Origin 6.0: Scientific Data Analysis and Graphing Software. www.originlab.com, 2000.
(29) Lu, T. Multiwfn. Software Manual, Version 2014, 2014.
(30) Alexander, S.; Orbach, R. Density of states on fractals: "fractons". *J. Phys. Lett.* **1982**, *43*, 625−631.
(31) Tenderholt, A. *PyMOlyze*, Version 1.1; Stanford University: Stanford, CA, 2006.
(32) (a) Shuai, Z.; Li, W.; Ren, J.; Jiang, Y.; Geng, H. Applying Marcus theory to describe the carrier transports in organic semiconductors: Limitations and beyond. *J. Chem. Phys.* **2020**, *153*, No. 080902. (b) Rashid, E. U.; Iqbal, J.; Mehmood, R. F.; El-Badry, Y. A.; Akram, S. J.; Khera, R. A. Depicting the role of end-capped acceptors to amplify the photovoltaic properties of benzothiadiazole core-based molecules

https://doi.org/10.1021/acsomega.2c07975
ACS Omega 2023, 8, 21425−21437

for high-performance organic solar cell applications. *Comput. Theor. Chem.* **2022**, *1211*, No. 113669.
(33) Hutchison, G. R.; Ratner, M. A.; Marks, T. J. Hopping transport in conductive heterocyclic oligomers: reorganization energies and substituent effects. *J. Am. Chem. Soc.* **2005**, *127*, 2339−2350.
(34) Rashid, E. U.; Hadia, N.; Alaysuy, O.; Iqbal, J.; Hessien, M.; Mersal, G. A.; Mehmood, R. F.; Shawky, A. M.; Khan, M. I.; Khera, R. A. Quantum chemical modification of indaceno dithiophene-based small acceptor molecules with enhanced photovoltaic aspects for highly efficient organic solar cells. *RSC Adv.* **2022**, *12*, 28608−28622.
(35) Zhou, J.; Wan, X.; Liu, Y.; Zuo, Y.; Li, Z.; He, G.; Long, G.; Ni, W.; Li, C.; Su, X.; Chen, Y. Small molecules based on benzo [1, 2-b: 4, 5-b′] dithiophene unit for high-performance solution-processed organic solar cells. *J. Am. Chem. Soc.* **2012**, *134*, 16345−16351.
(36) Qaisar, M.; Zahid, S.; Khera, R. A.; El-Badry, Y. A.; Saeed, M. U.; Mehmood, R. F.; Iqbal, J. Molecular Modeling of Pentacyclic Aromatic Bislactam-Based Small Donor Molecules by Altering Auxiliary End-Capped Acceptors to Elevate the Photovoltaic Attributes of Organic Solar Cells. *ACS Omega* **2022**, *7*, 20528−20541.
(37) Paramasivam, M.; Gupta, A.; Babu, N. J.; Bhanuprakash, K.; Bhosale, S. V.; Rao, V. J. Funnel shaped molecules containing benzo/pyrido [1, 2, 5] thiadiazole functionalities as peripheral acceptors for organic photovoltaic applications. *RSC Adv.* **2016**, *6*, 66978−66989.
(38) Salim, M.; Rafiq, M.; Khera, R. A.; Arshad, M.; Iqbal, J. Amplifying the photovoltaic properties of azaBODIPY core based small molecules by terminal acceptors modification for high performance organic solar cells: A DFT approach. *Sol. Energy* **2022**, *233*, 31−45.
(39) (a) Akram, S. J.; Iqbal, J.; Ans, M.; El-Badry, Y. A.; Mehmood, R. F.; Khera, R. A. Designing of the indacenodithiophene core-based small molecules for optoelectronic applications: A DFT approach. *Sol. Energy* **2022**, *237*, 108−121. (b) Azeem, U.; Khera, R. A.; Naveed, A.; Imran, M.; Assiri, M. A.; Khalid, M.; Iqbal, J. Tuning of a A−A−D−A−A-Type Small Molecule with Benzodithiophene as a Central Core with Efficient Photovoltaic Properties for Organic Solar Cells. *ACS Omega* **2021**, *6*, 28923−28935.
(40) Widmer, J.; Tietze, M.; Leo, K.; Riede, M. Open-circuit voltage and effective gap of organic solar cells. *Adv. Funct. Mater.* **2013**, *23*, 5814−5821.
(41) Farhat, A.; Khera, R. A.; Iqbal, S.; Iqbal, J. Tuning the optoelectronic properties of Subphthalocyanine (SubPc) derivatives for photovoltaic applications. *Opt. Mater.* **2020**, *107*, No. 110154.
(42) Zubair, I.; Kher, R. A.; Akram, S. J.; El-Badry, Y. A.; Saeed, M. U.; Iqbal, J. Tuning the optoelectronic properties of Indacenodithiophene based derivatives for efficient photovoltaic applications: A DFT Approach. *Chem. Phys. Lett.* **2022**, *793*, No. 139459.
(43) Saeed, M. U.; Iqbal, J.; Mehmood, R. F.; Akram, S. J.; El-Badry, Y. A.; Noor, S.; Khera, R. A. End-capped modification of Y-Shaped dithienothiophen [3, 2-b]-pyrrolobenzothiadiazole (TPBT) based non-fullerene acceptors for high performance organic solar cells by using DFT approach. *Surf. Interfaces* **2022**, *30*, No. 101875.
(44) Rafiq, M.; Salim, M.; Noreen, S.; Khera, R. A.; Noor, S.; Yaqoob, U.; Iqbal, J. End-capped Modification of Dithienosilole Based Small Donor Molecules for High Performance Organic Solar Cells Using DFT Approach. *J. Mol. Liq.* **2021**, No. 118138.
(45) (a) Palomo, L.; Favereau, L.; Senthilkumar, K.; Stępień, M.; Casado, J.; Ramírez, F. J. Simultaneous Detection of Circularly Polarized Luminescence and Raman Optical Activity in an Organic Molecular Lemniscate. *Angew. Chem., Int. Ed.* **2022**, *61*, No. e202206976. (b) Sharif, A.; Jabeen, S.; Iqbal, S.; Iqbal, J. Tuning the optoelectronic properties of dibenzochrysene (DBC) based small molecules for organic solar cells. *Mater. Sci. Semicond. Process.* **2021**, *127*, No. 105689.
(46) Rani, M.; Iqbal, J.; Mehmood, R. F.; Rashid, E. U.; Rani, S.; Raheel, M.; Khera, R. A.; et al. Strategies toward the end-group modifications of indacenodithiophene based non-fullerene small molecule acceptor to improve the efficiency of organic solar cells; a DFT study. *Comput. Theor. Chem.* **2022**, *1213*, No. 113747.
(47) Rafiq, M.; Khera, R. A.; Salim, M.; Khalid, M.; Ayub, K.; Iqbal, J. Tuning the optoelectronic properties of scaffolds by using variable central core unit and their photovoltaic applications. *Chem. Phys. Lett.* **2021**, *782*, No. 139018.
(48) Ans, M.; Paramasivam, M.; Ayub, K.; Ludwig, R.; Zahid, M.; Xiao, X.; Iqbal, J. Designing alkoxy-induced based high performance near infrared sensitive small molecule acceptors for organic solar cells. *J. Mol. Liq.* **2020**, *305*, No. 112829.
(49) Waqas, M.; Iqbal, J.; Mehmood, R. F.; Akram, S. J.; Shawky, A. M.; Raheel, M.; Rashid, E. U.; Khera, R. A. Impact of end-capped modification of MO-IDT based non-fullerene small molecule acceptors to improve the photovoltaic properties of organic solar cells. *J. Mol. Graphics Model.* **2022**, *116*, No. 108255.
(50) Guerra, C. F.; Handgraaf, J. W.; Baerends, E. J.; Bickelhaupt, F. M. Voronoi deformation density (VDD) charges: Assessment of the Mulliken, Bader, Hirshfeld, Weinhold, and VDD methods for charge analysis. *J. Comput. Chem.* **2004**, *25*, 189−210.
(51) Aslam, M. R.; Khera, R. A.; El-Badry, Y. A.; Rafiq, M.; Naveed, A.; Shehzad, M. T.; Iqbal, J. Tuning of diphenylamine subphthalocyanine based small molecules with efficient photovoltaic parameters for organic solar cells. *J. Mol. Graphics Model.* **2022**, *112*, No. 108146.
(52) Gruhn, N. E.; da Silva Filho, D. A.; Bill, T. G.; Malagoli, M.; Coropceanu, V.; Kahn, A.; Brédas, J.-L. The vibrational reorganization energy in pentacene: molecular influences on charge transport. *J. Am. Chem. Soc.* **2002**, *124*, 7918−7919.
(53) Yao, H.; Cui, Y.; Qian, D.; Ponseca, C. S., Jr.; Honarfar, A.; Xu, Y.; Xin, J.; Chen, Z.; Hong, L.; Gao, B.; et al. 14.7% efficiency organic photovoltaic cells enabled by active materials with a large electrostatic potential difference. *J. Am. Chem. Soc.* **2019**, *141*, 7743−7750.
(54) Akram, S. J.; Iqbal, J.; Mehmood, R. F.; Iqbal, S.; El-Badry, Y. A.; Khan, M. I.; Ans, M.; Khera, R. A. Impact of side-chain engineering on the A-π-D-π-A type SM-BF1 donor molecule for bulk heterojunction and their photovoltaic performance: A DFT approach. *Sol. Energy* **2022**, *240*, 38−56.
(55) Malmqvist, P. Å. Calculation of transition density matrices by nonunitary orbital transformations. *Int. J. Quantum Chem.* **1986**, *30*, 479−494.
(56) Luzanov, A. V.; Sukhorukov, A.; Umanskii, V. Application of transition density matrix for analysis of excited states. *Theor. Exp. Chem.* **1976**, *10*, 354−361.
(57) Gong, P.; Guo, P.; Wang, Y.; Yan, L.; Liang, Z.; Ding, M.; Tong, J.; Li, J.; Xia, Y. Ultrafast Kinetics Investigation of a Fluorinated-Benzothiadiazole Polymer with an Increased Excited State Transition Dipole Moment Applied in Organic Solar Cells. *ACS Appl. Energy Mater.* **2021**, *4*, 9627−9638.
(58) Duan, Y. A.; Geng, Y.; Li, H. B.; Jin, J. L.; Wu, Y.; Su, Z. M. Theoretical characterization and design of small molecule donor material containing naphthodithiophene central unit for efficient organic solar cells. *J. Comput. Chem.* **2013**, *34*, 1611−1619.
(59) Khan, M. I.; Hadia, N.; Iqbal, J.; Akram, S. J.; Hessien, M.; Shawky, A. M.; Aloui, Z.; Alatawi, N. S.; Khera, R. A. Novel A-π-D-π-A-type non-fullerene acceptors for solution-processed organic photovoltaic cells: A DFT study. *J. Solid State Chem.* **2023**, *317*, No. 123714.
(60) Rasool, A.; Zahid, S.; Ans, M.; Muhammad, S.; Ayub, K.; Iqbal, J. Bithieno thiophene-based small molecules for application as donor materials for organic solar cells and hole transport materials for perovskite solar cells. *ACS Omega* **2022**, *7*, 844−862.
(61) Zubair, I.; Khera, R. A.; Naveed, A.; Shehzad, R. A.; Iqbal, J. Designing the optoelectronic properties of BODIPY and their photovoltaic applications for high performance of organic solar cells by using computational approach. *Mater. Sci. Semicond. Process.* **2022**, *148*, No. 106812.
(62) Dang, M. T.; Hirsch, L.; Wantz, G. *P3HT:PCBM, Best Seller in Polymer Photovoltaic Research*; Wiley, 2011.
(63) Berthod, C.; Strandberg, R.; Yordanov, G. H.; Beyer, H. G.; Odden, J. O. On the variability of the temperature coefficients of mc-Si solar cells with irradiance. *Energy Procedia* **2016**, *92*, 2−9.
(64) Rajeswari, R.; Islavath, N.; Raghavender, M.; Giribabu, L. Recent progress and emerging applications of rare earth doped phosphor materials for dye-sensitized and perovskite solar cells: a review. *Chem. Rec.* **2020**, *20*, 65−88.

https://doi.org/10.1021/acsomega.2c07975
ACS Omega 2023, 8, 21425−21437